

Low And High Data Rate Transfer Switchable or Reconfigurable Filters

G. Keerthika¹, L.Kabila², R.Abinaya³, R.Revathi⁴

^{1,2,3,4}Dept of Electrical and Communication Engineering

^{1,2,3,4}K.Ramakrishnan college of Technology, Samayapuram, Trichy-621112

Abstract- This paper presents a systematic design procedure of four channels switchable or reconfigurable filter of higher order band pass filter with two transmission zeros (TZ) using source load coupling with minimum number of capacitor and inductor with minimum supply voltage. This filter has been designed in dash board or PCB board using soldering. This filter shows a good in –band and out of –band performance. This filter has high selectivity and low insertion loss. This filter has been experimentally demonstrated for both fourth and sixth order tunable filter.

I. INTRODUCTION

In modern multi standard wireless system require reconfigurable for multiband operation; therefore switchable or reconfigurable front end filters are in high demand.

An electronically controlled band pass filter (BPF) is one of the promising microwave components for future wireless communications. In recent years, therefore, the development of tunable BPFs having functionalities of continuous pass band-response controls, such as center frequency and frequency bandwidth, has become very active in microwave filter designs. In planar tunable filters using control elements, such as variable capacitors or varactor, tunable micro strip dual-mode filters have been developed to achieve a constant absolute frequency bandwidth (ABW), but the design techniques may be specialized for a shape of dual-mode resonator. To enhance frequency agilities, varactor diodes are additionally loaded at gaps between two adjacent micro strip resonators of a combine filter for the control of coupling coefficients. However, increasing the number of varactor diodes may lead to the increase of insertion loss at pass band and the increase of complexity for setting dc-bias voltages of varactor diodes. One of frequency agilities to be achieved by tunable filters is that only center frequency of pass band is tuned with varactors, maintaining a constant ABW of pass band.

In recent years decades, electrically tunable planar filters have received increasingly great attention from both the academic world and industry field, due to their ability to substantially reduce size for the multiband

transceiver front end and because of their high flexibility for cognitive/software defined radio . During this period, a large number of high-performance tunable filters were reported to provide possible solutions. However, achieving abroad frequency covering range (50%) is still a challenge for tunable filter design, especially with a constant bandwidth (BW). On the other hand, the emerging carrier aggregation system allows a total BW of up to 100-MHz mobile broadband wireless communications to meet the IMT-advanced requirements. Such a great expectation places an urgent demand on the wide tuning range dual-band tunable components. Unfortunately, the dual-band tunable filter with a broad tuning range as a promising solution has seldom been reported. This is because the sufficient stop band BW for the second pass band, and wide tuning range for two pass band are not easy to be achieved simultaneously.

II. OBJECTIVES

The goal of this paper is to implement a switchableOr reconfigurable four-channel band pass filter (BPF) bank with low loss and high selectivity. The filter bank was required to be configured to four different RF bands (i.e., 1–1.5, 1.5–2, 2–2.5, and 2.5–3 GHz), while the rejection level had to be higher than 20 dB in the stop band. The scores of each channel were judged by the following equation:

$$(m_4 + m_5) - 2 * (m_1 + m_2 + m_3),$$

Where m_1 , m_2 , and m_3 are the insertion losses at the center and at both sides of the pass band, while m_4 and m_5 are the rejection levels at each specific frequency respectively, meanwhile, the circuit was required to be compact and the final scores were calculated by the total scores of the four channels tfr4minus the circuit size.

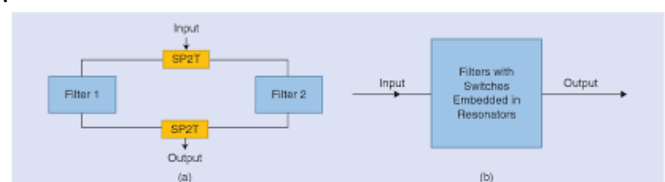


Figure 1 The four filter topologies investigated to meet the on-off-time requirement identified for the communication (a) two

Main block diagram of four channel filter design.

A. FILTER DESIGN

The tunable BPF is a suitable choice to achieve multichannel operation in a compact size.

However, it is not easy to implement a tunable filter with the wide tuning range of 1–3 GHz and a constant absolute bandwidth of 500 MHz. Tunable filters with two switch-selected channels can be used to achieve such a wide tuning range but at the cost of a high insertion loss introduced by the tunable components and switches. Recently, many switchable filter banks have been reported that achieve flexible reconfigurable functions with good performance.

We selected a switchable filter bank with four fixed channels for the competition, where two single-pole, four-throw (SP4T) switches are used for channel selection. A high-order BPF with source–load coupling is used to achieve high selectivity in each channel, while an additional transmission zero is allocated at the specific. The switchable filter bank could be composed of any type of lumped, planar, or cavity resonators for a channel filter design along with RF or Microwave switch circuits. The RF switches must be controlled electronically to make each channel state. RF switch could be any type of circuitry using solid state switches or RF relays. The filter bank must have female SMA connectors on the edges of the filter for the measurement. The filter will be evaluated based on the performance measured between the SMA connector interface reference planes. A network analyzer and two power voltage sources (0-20 Volts, 0-100 mA) will be available for measurements and filter reconfiguration. The filter bank size should be as small as possible. The size factor will be considered for the scoring. The total score will be calculated based on the following four filter specifications.

❖ Channel 1 :

- Pass band :1-1.5 GHz, Bandwidth 500 MHz
- Insertion loss: as low as possible
- Stop band : >20 dB for DC -0.75 GHz and 1.75 –3 GHz

❖ Channel 2 :

- Pass band :1.5 –2.0 GHz, Bandwidth 500 MHz
- Insertion loss: as low as possible
- Stop band : >20 dB for DC -1.25 GHz and 2.25 –3 GHz

❖ Channel 3 :

- Pass band :2.0 –2.5 GHz, Bandwidth 500 MHz
- Insertion loss: as low as possible
- Stop band : >20 dB for DC -1.75 GHz and 2.75 –4 GHz

❖ Channel 4 :

- Pass band :2.5 –3.0 GHz, Bandwidth 500 MHz
- Insertion loss: as low as possible
- Stop band : >20 dB for DC -2.75 GHz and 3.25 –4 GHz

Fig.1 Channel 1 estimated response: s21 (dB) reading will be rounded to the first decimal point at each marker frequencies.

➤ Ch.1 = [m4(46.4) +m5(31.0)]-2* [m1(4.0) + m2(1.5)+m3(3.5)] = 59.4

Fig.2 Channel 2 estimated response, s21 (dB) reading will be rounded to the first decimal point at each marker frequencies.

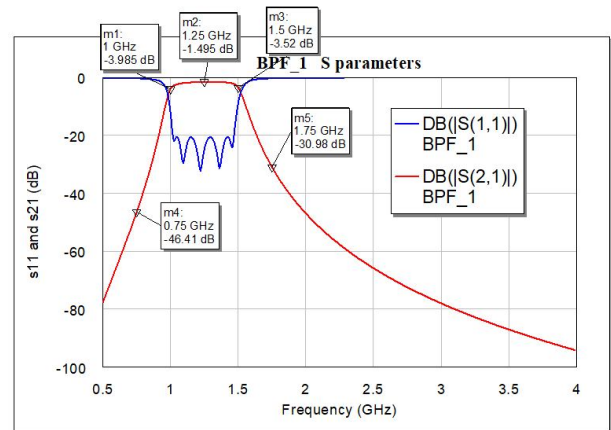
➤ Ch.2 = [m4(40.2) +m5(28.2)] -2* [m1(4.3) + m2(2.0)+m3(3.0)] = 49.8

Fig.3 Channel 3 estimated response, s21 (dB) reading will be rounded to the first decimal point at each marker frequencies.

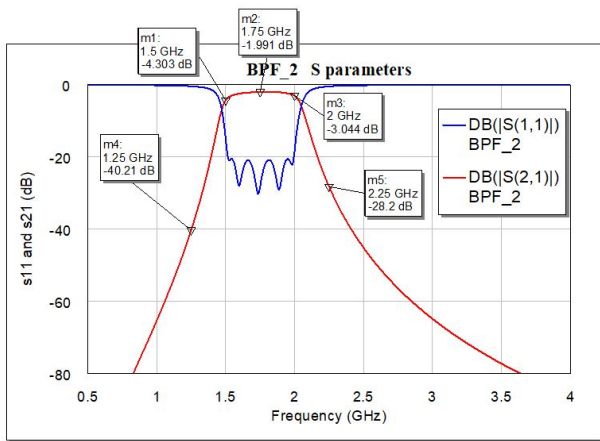
➤ Ch.3 = [m4(37.2) +m5(28.7)] -2*[m1(4.7) + m2(2.5)+m3(3.9)] = 43.7

Fig.4 Channel 4 estimated response, s21 (dB) reading will be rounded to the first decimal point at each marker frequencies.

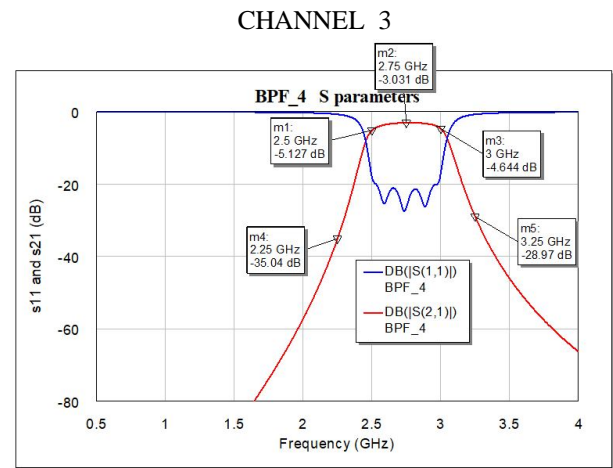
➤ Ch.4 = [m4(35.0) +m5(29.0)] -2* [m1(5.1) + m2(3.0)+m3(4.6)] = 38.6



CHANNEL 1



CHANNEL 2

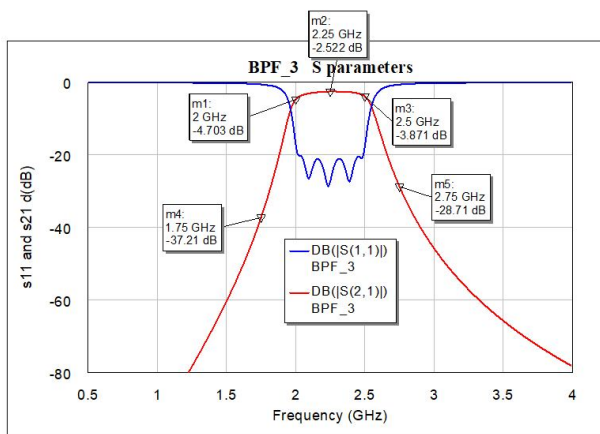


CHANNEL 4

High-Order BPF With Two Transmission Zeros Using Source–Load Coupling

In this competition, higher scores could be obtained by using a BPF with higher selectivity and lower loss. Here, high selectivity could be introduced by the high-order BPF. However, considering the relatively larger insertion loss of a high-order BPF at higher frequencies, two types of BPFs, i.e., fourth and sixth-order BPFs are used in the channels with higher and lower operation frequency, respectively. The coupling schemes of these BPFs, where the normalized coupling matrices of the required fourth-order BPF M_f and sixth-order BPF M_s with return loss lower than -20 dB are synthesized as;

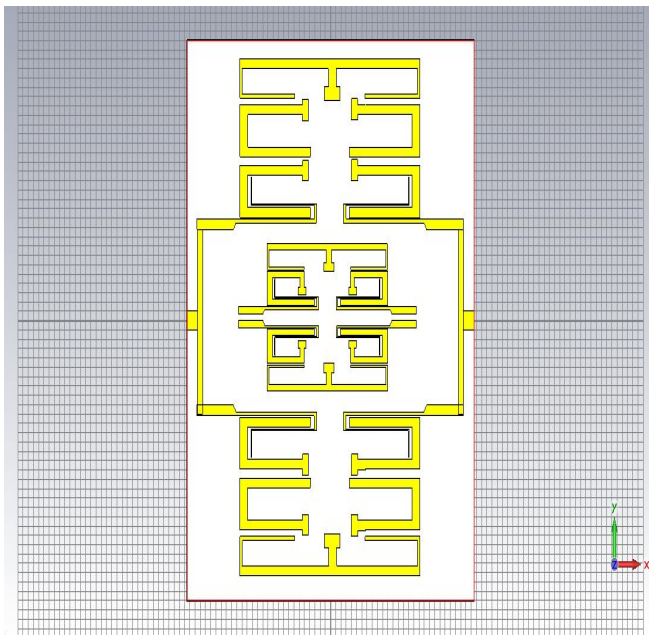
$$[M_s] = \begin{vmatrix} 0 & 1.030 & 0 & 0 & 0 & 1.030 \\ 1.030 & 0 & 0.880 & 0 & 0 & 0 \\ 0 & 0.880 & 0 & -0.716 & 0 & 0 \\ 0 & 0 & -0.716 & 0 & 0.880 & 0 \\ 0 & 0 & 0 & 0.880 & 0 & 1.030 \\ 0.070 & 0 & 0 & 0 & 1.030 & 0 \end{vmatrix}$$



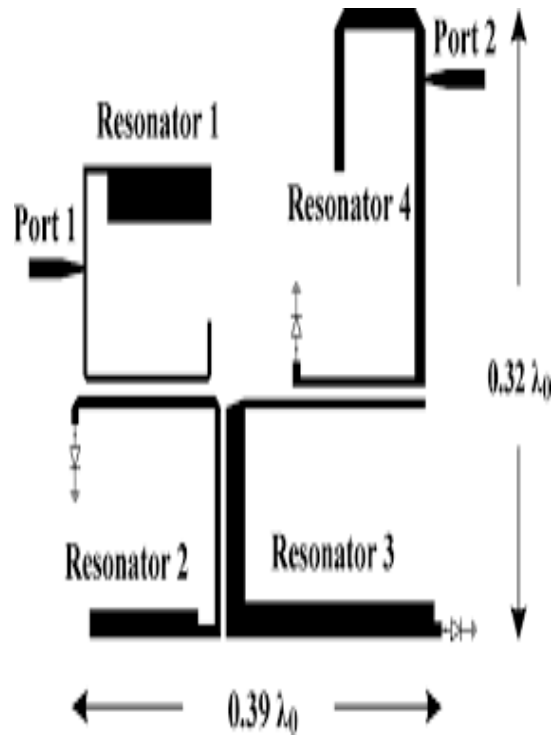
Here the values in the upper right and lower left of the matrices represent the normalized source–load coupling coefficients. Figure 3(a) and (b) shows the calculated frequency responses of the coupling matrices $[M_f]$ and $[M_s]$, where two transmission zeros (i.e., f_{z1} and f_{z2}) are located on both sides of the pass band.

The transmissions zeros can be adjusted by the source load coupling, while a higher selectivity can be obtained by introducing stronger source–load coupling. Next, the fourth- and sixth-order BPFs are implemented using $m/4$ resonators based on the aforementioned coupled schemes.

The layout of the proposed high-order BPF, where the $m/4$ resonators are folded for a compact size. Meanwhile, the square defected ground structures on the bottom layer are used to enhance the coupling strength between the two resonators. Here, two meander feed lines are in parallel with $m/4$ resonators as input–output ports. The source–load coupling is adjusted primarily by the gap between the two feed lines (i.e., $g/3$ and $W_s/9$ in the fourth- and sixth-order BPFs, respectively). Based on the structures mentioned, the lower channels (i.e., channels 1 and 2) and the higher channels (i.e., channels 3 and 4) are implemented with sixth- and fourth-order BPFs, respectively. To investigate the operation of the proposed structures, we used the Rogers 4350 dielectric substrate ($\epsilon_r = 3.66$; thickness $t = 0.508$ mm), an IE3D full-wave electromagnetic (EM) simulator, and the Advanced Design System design tool. Depicts the EM-simulated frequency response of the proposed high-order BPF in each channel. All the physical dimensions of the proposed filter banks. Here, the transmission zero f_{z2} is located in the upper stop band, which can achieve a high rejection level at the specific frequency by adjusting the source–load coupling strength. Meanwhile, the pass bands are optimized for low loss within the 500-MHz bandwidth.

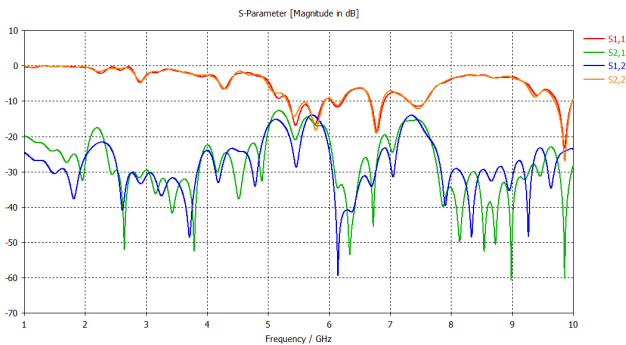


The layout designs which as obtained using proposed method.ch channel.



Fourth order switchable filter

Hence this filter can be design through mat lab through which the filters frequency can be obtained. This filter can be designed in cadence software hence layout design can be obtained though it. This filter consist of inductor, capacitor patch antenna (connected in both transmitter and receiver responsible for transmission), and switches.



The s-parameter which was obtained through proposed method.

Component	Channel 1	Channel 2	Channel 3	Channel 4
C_s	13 pF	6 pF	6 pF	6 pF
C_p	1 pF	0.7 pF	0.6 pF	0.3 pF
LP	36 nH	16 nH	10 nH	8.9 nH

Sixth-Order Filters												
	k_{11}	k_{12}	k_{13}	k_{14}	k_{15}	k_{16}	k_{17}	k_{18}	k_{19}	k_{20}	k_{21}	k_{22}
Channel 1	37.6	37.6	18.69	38.23	16.69	3.1	0.925	1.7	1.7	0	8.7	9.7
Channel 2	26.55	26.25	12.2	32.21	9.55	1.9	2.675	3.1	1.4	1.95	4.7	7.7
	k_{11}	k_{12}	k_{13}	k_{14}	W_{10}	W_{11}	W_{12}	W_{13}	W_{14}	W_{15}	W_{16}	W_{17}
Channel 1	10.7	11.9	11.4	11.9	0.55	0.35	0.2	0.18	0	0	0	0.2
Channel 2	8.7	8.9	8.9	8.9	0.65	0.45	0.3	0.2	0.1	1.8	1.15	0.5
	W_{18}	W_{19}	W_{20}	W_{21}	W_{22}	W_{23}	g_{11}	g_{12}	g_{13}	g_{14}	g_{15}	d
Channel 1	0.62	1.43	1.77	1.53	0.98	1.145	0.1	0.12	0.1	0.375	0.12	0.4
Channel 2	0.48	1.43	1.53	1.08	1.42	1.335	0.1	0.1	0.1	0.375	0.28	0.4
Fourth-Order Filters												
	k_{11}	k_{12}	k_{13}	k_{14}	k_{15}	k_{16}	k_{17}	W_{11}	W_{12}	W_{13}	W_{14}	
Channel 3	22.62	21.9	21.5	1.2	1.7	1.8	4.9	7.7	0.7	0.5	0.3	0.6
Channel 4	20.53	18.2	17.03	0.8	5.7	1.3	4.9	7.7	0.65	0.5	0.3	0.6
	W_{15}	W_{16}	W_{17}	W_{18}	W_{19}	W_{20}	g_{16}	g_{17}	g_{18}	g_{19}	g_{20}	d
Channel 3	0.5	0.13	0.3	0.1	0.28	0.96	0.13	0.1	0.12	0.49	0.415	0.4
Channel 4	0.5	0.15	0.3	0.1	0.3	0.8	0.1	0.1	0.12	0.44	0.4	0.4

The physical dimensions of four channels

TABLE 3. A comparison with state-of-the-art switchable filter banks.				
	[4]	[14]	[15]	This Work
Topology	Varactor tuned and switchable	Switchable	Varactor tuned and switchable	Switchable
Number of channels	2	2	2	4
Operating frequency range	0.76–2.63 GHz	2.4–2.5 GHz 4.2–4.4 GHz	0.36–0.97 GHz	1–3 GHz
Insertion loss	2–4.78 dB	4–5 dB*	3.6–5.8 dB	2.7–4.2 dB
Selectivity	High	Medium	Low	High
Size ($\lambda_x \times \lambda_y$)	$0.33 \times 0.11^*$	0.63×0.63	0.13×0.11	0.29×0.34

A comparison with state-of-the-art switchable filter bank.

Cascaded Static BSF without Disturbing the Pass band

A static BSF is introduced and cascaded with the high order BPF to further enhance the selectivity of the lower stop band; the BSF consists of two capacitors (i.e., C_p and dc-block capacitor C_s) and one inductor L_p . The operation frequency of the BSF (i.e., f_0) can be calculated as follows:

$$f_0 = 1 / (2\pi(L * C)^{1/2}).$$

In addition, the bandwidth of the BSF can be adjusted by tuning the ratio K of the inductance L_p to the capacitance C_p . Due to the limited unloaded quality factor (Q_u) of practical lumped elements, a higher attenuation level at the center frequency can be achieved by increasing the bandwidth of the BSF.

Therefore, there is a tradeoff between the attenuation level and the in-band insertion loss, since the wideband BSF response will cause the adjacent pass band performance to degenerate. The bandwidth of the BSF could be finely controlled to maximize the attenuation level, which shows negligible influence on the pass band of the high-order BPF. The values of the inductor L_p and capacitor C_p can be calculated once the operating frequency and bandwidth of the BSF are determined. Here, we used the high-Q GJM and LQW series capacitors and inductors from Murata in the static BSF of each channel.

The relatively high insertion loss is primarily caused by the two switches, while the discrepancy between simulation and measurement is primarily due to manufacturing tolerance.

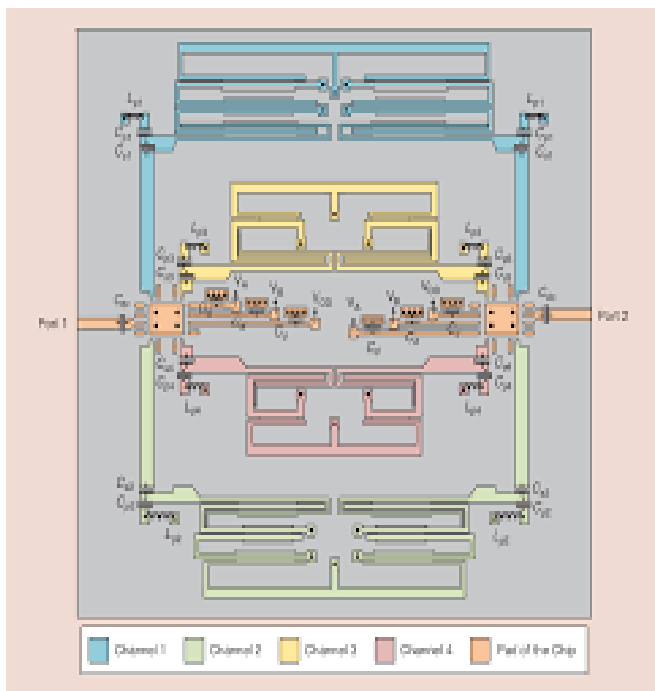


Figure 7. The layout of the implemented four-channel switchable filter bank.

The layout implementation of four channel filter in base paper.

Implementation and Measured Results

Filter Bank Implementation Using SP4T

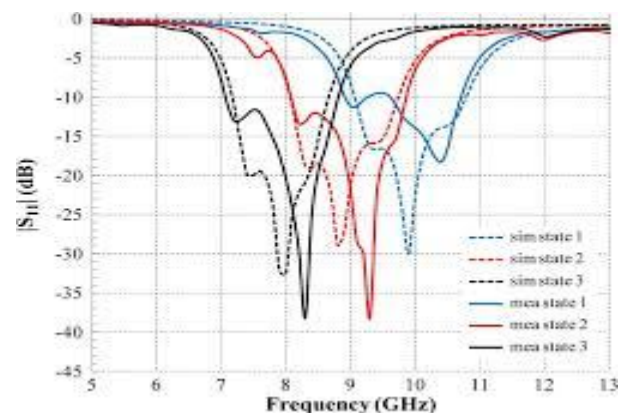
To implement our device, we used HMC241ALP3E SP4T switches from Analog Devices for channel selection. Each switch is controlled by two logic input voltages VA and VB, while the 3.5-V supply voltage is fed by a VDD pin. Figure 7 shows the layout of the implemented filter, where C_d and C_{dc} are the decoupling and dc-blocking capacitors, respectively.

The Performance of the Manufactured

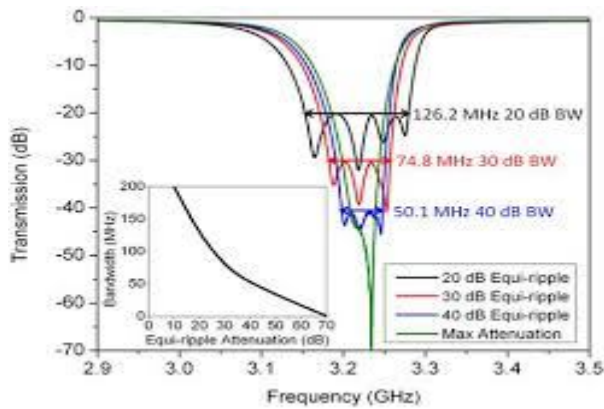
Four-Channel Switchable Filter Bank

The size of the fabricated filter bank is 50×60 mm (i.e., 0.29×0.34 mg , where mg is the micro strip-guided wavelength at 1.25 GHz). Here, two inverters are used to reduce the number of control voltages. Measurement was performed by the Agilent 5230 A network analyzer. As shown in Figure, the measured insertion losses of channel 1–4 are 2.7–3.8, 3–4, 2.8–3.9, and 3.1–4.2 dB, respectively.

Meanwhile, good in-band group delays are measured with a return loss of better than -10 dB in all channels. The relatively high insertion loss is primarily caused by the two switches, while the discrepancy between simulation and measurement is primarily due to manufacturing tolerance. A comparison of the proposed filter with the state of the art as shown in table which reveals that this switchable filter bank features high selectivity and lower insertion loss in multiple channels.



Performance of switchable filter.



Tunable filter frequency response.

III. CONCLUSIONS

We designed, built, and tested a four-channel switchable filter bank using a high-order BPF and SP4T for channel selection. Static BSFs were introduced for selectivity enhancement. The implemented filter bank is capable of switching between four different channels operated at 1–1.5, 1.5–2, 2–2.5, and 2.5–3 GHz, respectively. As it satisfied all of the requirements of the competition rules and showed good in-band and out-of-band performance, this design won first place in the IMS 2019 SDC. Because it demonstrated such good performance, the designed filter is likely to be an attractive choice for multi standard wireless communication applications.

REFERENCES

- [1] IEEE Microwave Theory and Techniques Society, "Student Design Competition Submission Form for Technical Committees." Accessed on: Oct. 2019. [Online]. Available: http://imsieee.org/sites/ims2019/files/content_images/IMS2019_SDC_call_for_proposals_Rev_A.pdf
- [2] R. Gomez Garcia, J. Muñoz-Ferreras, and D. Psychogiou, "Fully reconfigurable band pass filter with static couplings and intrinsic switching capabilities," in Proc. IEEE MTT-S Int. Microwave Symp., Honolulu, HI, June 2017, pp. 914–917.
- [3] M. Ohira, S. Hashimoto, Z. Ma, and X. Wang, "Coupling-matrix based systematic design of single-dc-bias-controlled micro strip higher order tunable band pass filters with constant absolute bandwidth and transmission zeros," IEEE Trans. Microwave Theory Tech., vol. 67, no. 1, pp. 118–128, Jan. 2019.
- [4] D. Lu, X. Tang, N. S. Barker, and Y. Fang, "Single-band and switchable dual-/signal-band tunable BPFs with predefined tuning range, bandwidth, and selectivity," IEEE Trans. Microwave Theory Tech., vol. 66, no. 3, pp. 1215–1227, Mar. 2018.
- [5] C.-F. Chen, G.-Y. Wang and J.-J. Li, "Micro strip switchable and fully tunable band pass filter with continuous frequency tuning range, IEEE Microwave. Wireless Compon. Lett. vol. 28, no. 6, pp. 500–502, June 2018.
- [6] R. Zhang, R. Gomez Garcia, and D. Peroulis, "Multifunctional band pass filters with reconfigurable and switchable band control," IEEE Trans. Microwave Theory Tech., vol. 67, no. 6, pp. 2355–2369, June 2019.
- [7] J. Xu, "Compact switchable band pass filter and its application to switchable diplexer design," IEEE Micro Wireless Compon. Lett. vol. 26, no. 1, pp. 13–15, Jan. 2016.
- [8] M. Z. Koochi and A. Mortazawi, "Compact intrinsically switchable filter bank employing multifunctional ferroelectric BST," in Proc. IEEE MTT-S Int. Microwave Symp., Philadelphia, PA, June 2018, pp. 849–851.
- [9] X. Luo, B. Yang, and H. J. Qian, "Adaptive synthesis for resonator-coupled filters based on particle swarm optimization," IEEE Trans. Microwave Theory Tech., vol. 67, no. 2, pp. 712–725, Feb. 2019.
- [10] R. Garg, I. Bahl, and M. Bozzi, Micro strip Lines and Slot lines, 3rd ed. Norwood, MA: Artech House, 2013.
- [11] Z. Deng, Z. Tian, H. J. Qian, and X. Luo, "A metamorphosed roadway: Dual-band variable-attenuation notch filters," IEEE Micro. Mag., vol. 19, no. 2, pp. 70–76, Mar. 2018.
- [12] Murata, "GJM1555x and LQW15x series datasheet," 2019. [Online]. Available: www.murata.com.
- [13] Analog Devices, "HMC241ALP3E," 2019. [Online]. Available: <https://www.analog.com/media/en/technical-documentation/data-sheets/hmc241alp3e.pdf>.
- [14] D. Shojaei-Asanjan and R. R. Mansour, "The sky's the limit: A switchable RF-MEMS filter design for wireless avionics intra communication," IEEE Micro. Mag., vol. 18, no. 1, pp. 100–106, Jan. 2017.
- [15] M. Jung and B. Min, "A compact tunable band pass filter using switchable varactor-tuned dual-mode resonator," in Proc. IEEE MTT-S Int. Microwave Symp., Philadelphia, PA, June 2018, pp. 1374–1377.